Journal of Engineering Physics and Thermophysics, Vol. 79, No. 5, 2006

NUMERICAL SIMULATION OF VISCOUS FLOW AROUND A SYSTEM OF BODIES ON THE BASIS OF THE NAVIER–STOKES EQUATIONS IN STREAM FUNCTION–VORTICITY VARIABLES

A. B. Mazo

UDC 532.516

A method of numerical solution of the Navier–Stokes equations in stream function–vortex–pressure variables is suggested to be used in simulating a nonstationary, nonsymmetric flow of a laminar incompressible viscous stream around a pair of rotating cylinders in a channel. Results of calculations which illustrate application of the method under different conditions of flow around bodies are presented.

Introduction. Separating flows near single blunt bodies and their systems continue to attract the attention of researchers. On the one hand, this is explained by practical interests since this class of flows is associated with diverse engineering problems — from calculation of tubular heat exchangers to designing bridges and offshore oil platforms. On the other hand, theoretical interest in the very phenomenon of periodic flow stalling from the surface of a body immersed in a flow to formation and development of complex vortical structures in the wake has not waned.

The simplest mathematical and numerical models of such flows are based on the Navier–Stokes two-dimensional equations, which adequately describe the hydrodynamics of a laminar flow at low and moderate Reynolds numbers. The fullest coverage in the literature has been provided for experimental and numerical results of investigation into an infinite separated flow of a viscous, incompressible fluid past a single fixed circular cylinder. However, recently publications have appeared concerned with the study of flow past a system of cylindrical bodies at Reynolds numbers lying in the range $40 < \mathrm{Re} < 200$. Thus, in the reviews of experimental works [1–3], characteristic features of a flow past a pair of fixed circular cylinders located at different distances from one another and differently orientated to the flow are presented. To carry out numerical simulation of this class of flows, different approaches have been suggested: from the method of discrete vortices [4] to a hybrid method of boundary and finite elements [5, 6]. As a rule, the results of calculations agree satisfactorily with experimental data. At the same time, an analysis of the literature shows that by no means have all the aspects of flow past a system of bodies been adequately studied, and development of alternative methods to perform numerical simulation in the given region remains of current interest.

Below, a nonstationary, nonsymmetrical laminar flow of an incompressible viscous fluid past a pair of rotating cylinders in a channel is considered. This statement generalizes the problem [7] of flow near a single cylinder with a rotational degree of freedom in a channel without friction on its walls. A method to numerically solve the Navier–Stokes equations in stream function–vortex–pressure variables that is based on the theoretical concepts presented in [8] is suggested.

Statement of the Problem. The dimensionless Navier–Stokes equations in the stream function ψ–vorticity ω variables have the form

$$\frac{\partial \omega}{\partial t} + u \frac{\partial \omega}{\partial x} + v \frac{\partial \omega}{\partial y} = \frac{1}{\mathrm{Re}} \Delta \omega , \quad x, y \in D ; \tag{1}$$

$$\Delta \psi = - \omega , \quad \omega = \frac{\partial v}{\partial x} - \frac{\partial u}{\partial y} , \quad u = \frac{\partial \psi}{\partial y} , \quad v = - \frac{\partial \psi}{\partial x} , \tag{2}$$

Institute of Mechanics and Machine Building, Kazan' Scientific Center, Russian Academy of Sciences, 2/31 Lobachevskii Str., Kazan', 420111, Russia; email: amazo@ksu.ru. Translated from Inzhenerno-Fizicheskii Zhurnal, Vol. 79, No. 5, pp. 118–125, September–October, 2006. Original article submitted February 9, 2005.

where u and v are the components of the velocity vector $\mathbf{V}$, with the average value of the longitudinal velocity u being equal to unity and the Reynolds number Re being based on the radius of one of the bodies immersed in a flow. The field of pressure p can be calculated at any fixed moment of time t if the functions ψ and ω are known at this time. The equation for the pressure is traditionally written in the form [9]

$$\Delta p = -2\left(\frac{\partial v}{\partial x}\frac{\partial u}{\partial y} - \frac{\partial u}{\partial x}\frac{\partial v}{\partial y}\right) = 2\left[\frac{\partial^2 \psi}{\partial x^2}\frac{\partial^2 \psi}{\partial y^2} - \left(\frac{\partial^2 \psi}{\partial x \partial y}\right)^2\right], \tag{3}$$

however, in [10] an alternative formulation of the problem for the Bernoulli variable B was suggested; it can be rearranged to the form [7]

$$-\Delta B = \text{grad}\,\omega\,\text{grad}\,\psi - \omega^2\,, \quad p = B - V^2/2\,. \tag{4}$$

From the viewpoint of numerical solution, the advantage of Eq. (4) over Eq. (3) is that to calculate the right-hand side of Eq. (4) it is sufficient to take the first derivatives of the grid solution of ψ and ω, whereas in Eq. (3) one has to find the second-order derivatives of the approximate solution of Eq. (2).

As the calculation region D, one selects a plane channel which is bounded by horizontal walls $y = \pm H$, inlet vertical section $x = -L_1$, outlet section $x = L_2$, and by inner boundaries γ_i, $i = 1, 2, \ldots, N$, which are the surfaces of N cylindrical bodies of unit radius placed into the channel. It is assumed that all the boundaries are impermeable and the channel walls are immovable, whereas the bodies can rotate; therefore the tangential velocities v_i at boundaries γ_i generally differ from zero. At the inlet to the channel, a stationary parabolic velocity profile is assigned:

$$u_0 = 1.5\,(1 - z^2)\,, \quad z = y/H$$

as well as the corresponding distributions of the stream function and vorticity; the pressure is assumed to be equal to zero. The boundary conditions at the inlet to the channel have the form

$$x = -L_1: \quad \psi = \psi_0 = 1.5H\,(1 + z)\left(1 - \frac{1 - z + z^2}{3}\right), \quad \omega = \omega_0 = \frac{3z}{H}\,, \quad B = \frac{u_0^2}{2}\,. \tag{5}$$

We note that the average velocity of the incoming flow is equal to unity, whereas the fluid flow rate in the channel is equal to $Q = \psi(H) - \psi(-H) = 2H$. In the outlet section of the channel, "mild" boundary conditions are set:

$$x = L_2: \quad \frac{\partial \psi}{\partial n} = 0\,, \quad \frac{\partial \omega}{\partial n} = 0\,, \quad \frac{\partial B}{\partial n} = \frac{\partial p}{\partial n} - u\frac{\partial u}{\partial n} \approx -\frac{1}{\text{Re}}\frac{\partial^2 u_0}{\partial y^2} = \frac{-3}{\text{Re}\,H^2} << 1\,. \tag{6}$$

In writing (6) for the Bernoulli variable, the assumption that $L_2 >> 1$ is adopted, so that the flow near the outlet boundary is close to a stationary one.

The problem of posing boundary conditions on surfaces immersed in a flow for Eqs. (1), (2), and (4) has been investigated in detail in [8]. Each of these boundaries is a streamline, but only on the channel walls are the values of $\psi(-H) = 0$ and $\psi(H) = Q$ known, whereas on the inner boundaries γ_i the values of the stream function are determined with the aid of a system of auxiliary harmonic functions η_i from the formulas

$$\psi_i = \frac{1}{|\gamma_i|}\left(\sum_{k=1}^{N} v_k \int_{\gamma_k} \eta_i ds - Q \int_{\Gamma_{\text{top}}} \frac{\partial \eta_i}{\partial n} ds + \int_D \eta_i \omega dD\right), \quad i = 1, 2, \ldots, N\,. \tag{7}$$

Here, $|\gamma|$ is the length of the contour γ; ds is an element of the arc length; Γ_{top} denotes the upper wall of the channel, and the direction of traverse along the boundaries during integration in (7) is selected so that the region could remain on the right. The auxiliary functions $\eta_i(x, y)$ satisfy the boundary-value problems

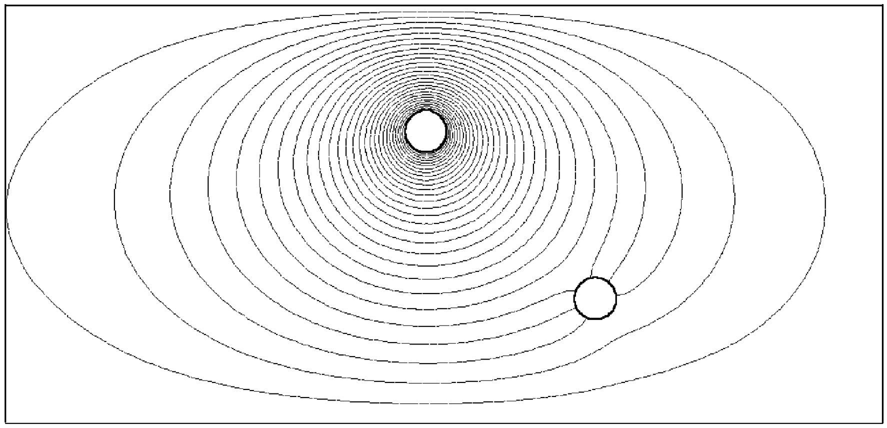

Fig. 1. Auxiliary function η_1 for the case of a flow around two cylinders.

$$\Delta\eta_i = 0\,,\quad x, y \cup D\,,\quad i = 1, 2, \ldots, N\,;$$
$$x = -L_1, L_2\,;\quad x, y \cup \gamma_{2,\ldots,N}:\ \frac{\partial\eta_i}{\partial n} = 0\,;\quad y = \pm H:\ \eta_i = 0\,;\quad x, y \cup \gamma_i:\ \frac{\partial\eta_i}{\partial n} = 1\,. \tag{8}$$

Relations (7) are considered as the main boundary conditions for Eq. (2) on the inner boundaries γ_i, whereas the Neumann conditions $\partial\psi/\partial n = v_i$ are used to determine the boundary values of vorticity. In [8], the following integral identity is used for this purpose:

$$\int_D \omega\eta dD = \int_D \nabla\psi\cdot\nabla\eta dD - \sum_{i=1}^{N}\int_{\gamma_i} v_i\eta ds\,, \tag{9}$$

in which η is an arbitrary trial function, whereas the stream function ψ on the right side is the solution of Eq. (2) with boundary conditions (7). The trace of the solution of problem (9) on the inner boundaries γ_i as well as on the channel walls is used as the Dirichlet boundary conditions for the problem of vorticity transfer (1). Finally, the boundary conditions for the Bernoulli variable on surfaces immersed in a flow are obtained from Pearson's relation [9], and, after generalization to the case of movable boundaries, they take the form

$$x, y \in \gamma_i:\ \frac{\partial B}{\partial n} = \frac{1}{\mathrm{Re}}\frac{\partial\omega}{\partial s} - v_i\omega\,. \tag{10}$$

Condition (10) is valid also on the channel walls, if it is assumed that there $v_i = 0$.

The system of relations (1), (2), (4)–(7), (9), and (10) represents a closed mathematical model of a viscous laminar flow past a system of rotating cylinders in a channel.

Algorithm of Numerical Solution. The solution of the problem begins from construction of a grid of triangular linear finite elements and renumbering its nodes with the aid of a minimum-degree algorithm to reduce the filling of the matrix when it is decomposed into triangular factors. Hereinafter, problems (8) are solved by a direct method to determine auxiliary functions η_i. The result for the case $N = 2$ is shown in Fig. 1. The calculation of η_i is followed by calculation of the first two integrals in formulas (7), and thereafter a change in the constants ψ_i is determined only by a change in ω in the last integral of (7).

At $t = 0$, the initial distribution of the vortex $\omega = \omega_0(x, y)$ is given (see Eq. (5)) and approximate values of streamlines $\psi_i^0 = \psi_0(y_i^c)$. Thereupon, in the time cycle $t_j = j\tau$, $j = 1, 2, \ldots$, the functions ψ and ω are calculated. The iteration scheme of solving the problem on the time layer is as follows:

1. The integrals over the region D of the product $\omega\gamma_i$ are calculated and, using Eq. (7), new values of the stream function at the boundaries γ_i are calculated.

2. The found values of ψ_i are used as boundary conditions in solving problem (2) for the stream function ψ. The grid scheme of finite elements is constructed on the basis of the integral identity

$$\int_D \nabla\psi\cdot\nabla\eta dD = \int_D \omega\eta dD \, . \tag{11}$$

The transition from (11) to finite-dimensional schemes is accomplished following a standard procedure; the basic boundary conditions are taken into account on the matrix level: in each line of the matrix of the system of equations that corresponds to the grid node with the Dirichlet conditions, the number $G >> 1$ is placed on the principal diagonal and the right side is multiplied by G.

3. The resulting distribution of the stream function is used to calculate the vortex at the boundary by solving problem (9). The approximating equation has the form $\mathbf{M}\omega = \mathbf{\Lambda}\psi + \mathbf{f}$, where $\mathbf{M}$ is the "sparse" symmetrical matrix within conditionality of the order of unity; $\mathbf{\Lambda}$ is the grid analog of the Laplace operator with the Neumann boundary conditions; the vector $\mathbf{f}$ is produced by the last term on the right side of Eq. (9), and it differs from zero only on the movable boundaries. The boundary values of the solution found are used as the Dirichlet conditions for the vortex.

4. Problem (1) is solved, and, after discretization in time, it has the form

$$\omega - \frac{\tau}{\mathrm{Re}}\Delta\omega = \phi\,(\psi, \omega, \omega^{j-1})\,, \quad \phi\,(\psi, \omega) = \omega^{j-1} - \tau\left(\frac{\partial\psi}{\partial y}\frac{\partial\omega}{\partial x} - \frac{\partial\psi}{\partial x}\frac{\partial\omega}{\partial y}\right),$$

where the last term on the right side is calculated from the values of the desired functions at the previous iteration. The spatial discretization of the problem for ω, just as the remaining grid approximations, are constructed on the basis of the integral identity

$$\int_D \omega\eta dD + \frac{\tau}{\mathrm{Re}}\int_D \nabla\omega\cdot\nabla\eta dD = \int_D \phi\eta dD \, . \tag{12}$$

The iterations are completed as soon as a further refinement of the constants ψ_i becomes unessential. Usually, the convergence with an accuracy of the order of 10^{-4} is attained in 8–10 iterations on each time layer. However, special numerical experiments have shown that during flow in a channel, fluctuations of the values of ψ_i caused by periodic vortex shedding have an amplitude an order of magnitude smaller (of the order of 10^{-4}) than in the problems of external flow past a body [7]. Therefore, the problem is solved in two stages. In the first stage, calculations are performed following the complete scheme described above, but for a short interval of time (usually no more than 100 steps). In this interval of time, the values of the constants ψ_i are being found. In the second stage, the stream functions found on the boundaries are fixed, and further calculation is performed without internal iterations.

The solution of the systems of algebraic equations produced by integral identities (9), (11), and (12) is performed by a direct method, with the Kholetskii factorization being made once, whereas in the internal iterative process and in passing to a new time layer only the right sides of the equations are renewed. To preserve the vectors and matrices, and also as for operations with these objects, the technique of the algebra of sparse matrices is used.

Having found the functions ψ and ω for a fixed t, it is possible to solve Eq. (4) and determine the Bernoulli variable $B(x, y)$ at this instant of time. In [11], the difficulties of solving the problem for pressure that were caused by the necessity of differentiating an approximate solution when calculating the right side of the equation and by the large length of the calculation region $L = L_1 + L_2 >> 1$ were noted. This can be illustrated by a simple example that preserves the problem properties discussed. We will consider the equation $b'' = \varphi$, $x \cup (0, L)$ with boundary-value conditions $b(0) = 0$ and $b'(L) = 0$, which are similar to conditions (5) and (6). At $\varphi = \mathrm{const}$, the solution has the form $b = \varphi L^2\xi(\xi/2 - 1)$, $\xi = x/L$. If the right side of the equation is prescribed with an error $\tilde{\varphi} = \varphi + \varepsilon$, then the maximum error of the solution will evidently be equal to $\varepsilon L^2/2$. The numerical experiments for problem (4)–(6), (10) have confirmed that variations of the right side of the equation at $\varepsilon \sim 10^{-3}$ and $L \sim 100$ lead to deviations of the calculated pressure of the order of 10. To reduce the error, the accuracy of the scheme of finite elements is raised as described in [11]. Based on the initial grid, a new grid of 10-nodal finite elements of third degree is constructed, and linear filling-in of the function ω is determined. Then, the equation $\Delta\psi = -\omega$ is solved on the new grid, and equations of dif-

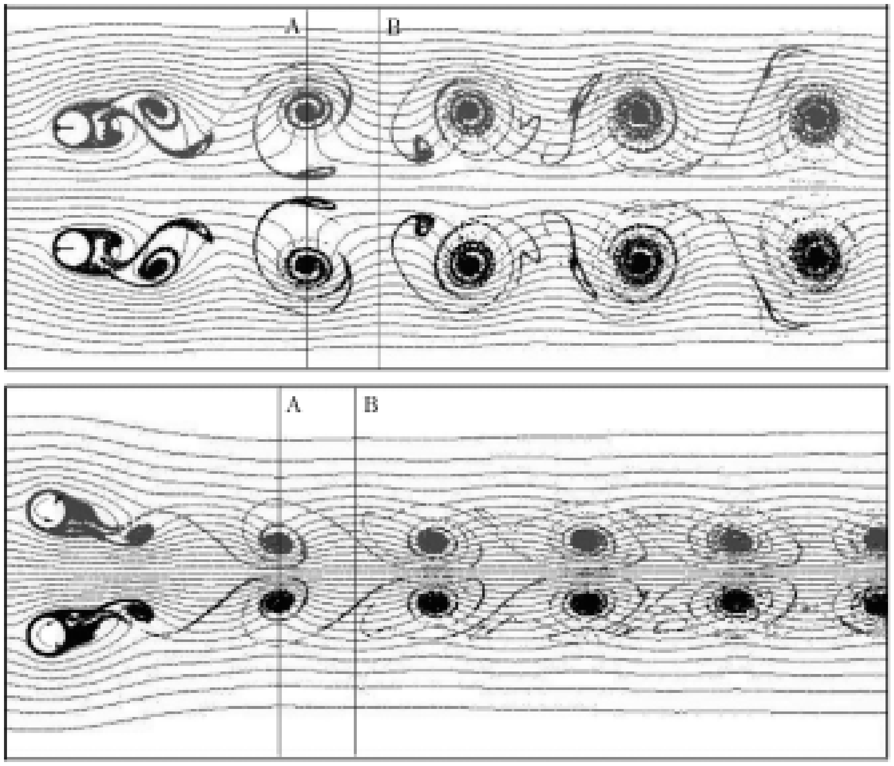

Fig. 2. Influence of rotation on the flow around a pair of cylinders located vertically in a channel at Re = 150; arrows on the lower picture show the directions of rotation; A and B, section in which velocity profiles differ substantially.

ferentiation are carried out to calculate the right side of Eq. (4). The boundary-value problems for ψ and B are solved by the method of conjugate gradients with a preconditioning operator constructed with the aid of a complete Kholetskii expansion.

Results of Simulation. In this section, some of the results of numerical simulation of a viscous flow past a pair of circular cylinders in a channel with boundaries $y = \pm H$, $H = 10$; $x = -L_1 = -30$, and $x = L_2 = 80$ are presented. The following cases were considered: cylinders located along the line of flow (in tandem), across the channel axis (vertically), and at an angle of 45^{o} to the axis (a diagonal scheme). In all calculations, Re = 150; the cylinders are modeled as both being immovable ($v_i = 0$) and with different directions of rotation ($v_i = \pm 1$).

Figure 2 depicts a symmetrical picture of flow downstream of a pair of cylinders located vertically. In the absence of rotation (upper figure), the bodies divide the incoming flow into the parts $\psi_1 = 7.1$ and $\psi_2 = 12.9$; when they rotate inside (lower picture), the values of the streamlines on the surfaces in a flow change to $\psi_1 = 5.5$ and $\psi_2 = 14.5$. In both cases, nearly a symmetrical structure of flow with an alternating change in the velocity profile in the transverse sections A and B is formed (Fig. 3).

On the whole, the rotation of the cylinders into the flow leads to the expected increase in the velocity in the flow core and its retardation near the channel walls. It should be noted that in sections A, where the vorticity concentration is observed, the redistribution of the flow from the axial line to the periphery occurs in the case of the immovable cylinders, whereas in the case of rotating bodies there is a relative flow acceleration in the flow core. This corresponds entirely to different directions of the rotation of vortices in the given sections (see Fig. 2).

The symmetrical picture of flow around the cylinders is disturbed when the latter are located diagonally. Figure 4 presents the streamlines in the vicinity of a pair of circular cylinders rotating in the direction from the axial line to the channel walls. Such a rotation leads to a substantial redistribution of flow rates between the surfaces of the bodies immersed in the flow: $\psi_1 = 9.46$ and $\psi_2 = 10.54$. These values show that only about 5% of the fluid passes between the cylinders, whereas the main part of the flow moves around the periphery; actually, in the given case there is an external flow past one movable "body" formed by the pair of cylinders with attached pulsed vortices. This is

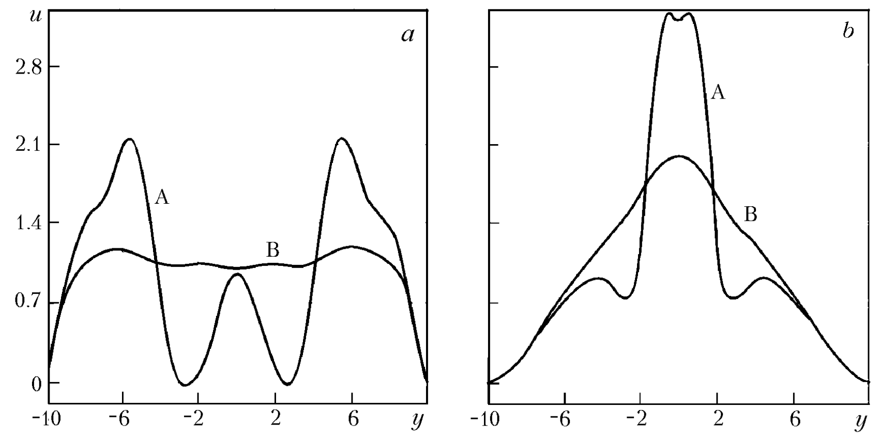

Fig. 3. Longitudinal velocity profiles in sections A and B (see Fig. 2) for an immovable pair of cylinders (a) and a pair of cylinders rotating into the flow (b).

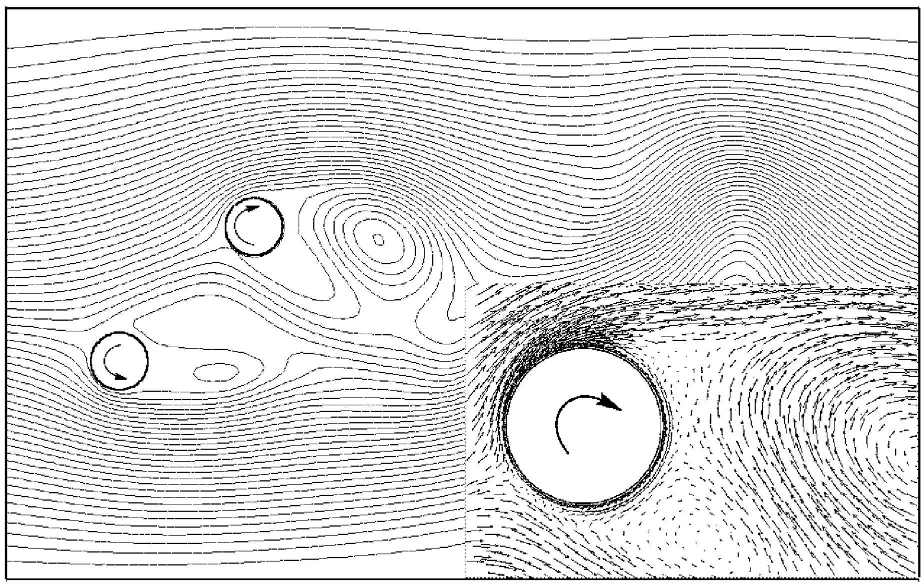

Fig. 4. Nonsymmetrical picture of streamlines in the case of diagonal location of cylinders rotating in the directions toward the channel walls; velocity field near the moving surface of a body.

also confirmed by the fact that the von Kármán streets downstream of the cylinders rapidly lose their individuality, and at a distance of $x \sim 40$ a common vortex wake is formed.

Next, we will consider the dynamics of flow around a tandem of immovable circular cylinders, with the distance between their centers equal to 6.667. From Fig. 5 it is seen that first independent paired vortices are formed downstream of each of the bodies immersed in the flow (the upper photograph on the left). With time, the eddy zone behind the first cylinder expands and practically "screens" the cylinder located downstream. The streamline emanating from the point of separation of the boundary layer of the preceding cylinder is attached to the frontal surface of the rear cylinder. Thus, a closed cavity with a circulating fluid is formed between the pair of the tandem. The pressure in the bottom region of the first cylinder is lowered, and this leads to the appearance and development of a reverse jet from the frontal point of the rear cylinder (the third and fourth photographs). Simultaneously, the instability and destruction of the symmetrical structure of the second vortex wake begin to manifest themselves, while the vertical cavity between the bodies remains stable and symmetrical. This process ends with formation of a single pulsating vortex wake downstream of the tandem. However, calculations show that the amplitude of the self-oscillations of the flow is low enough to allow us to speak of a "separationless" flow around the tandem of cylinders with a vortical cavity be-

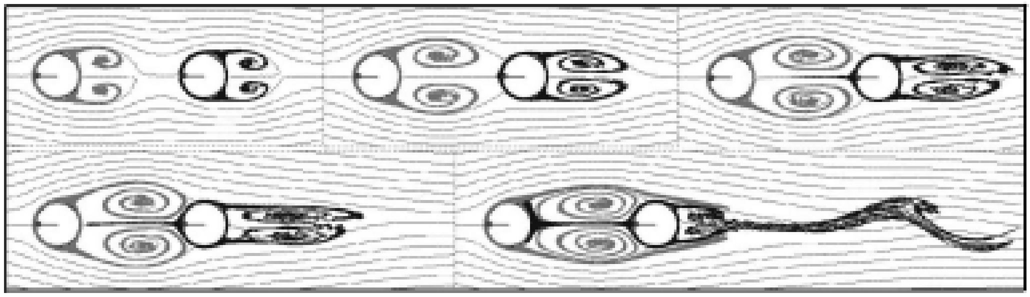

Fig. 5. Development of vortex structures in a stream flowing around a tandem of circular cylinders at Re = 150.

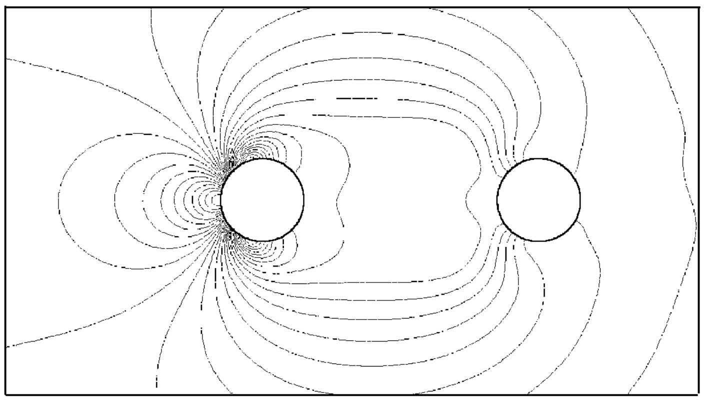

Fig. 6. Pressure field in a stream flowing around a tandem of circular cylinders at Re = 150.

tween them. The role of this cavity in the formation of the flow structure seems to be analogous to the effect of eddy cells on the aerodynamic profiles studied in [12].

The pressure field in the vicinity of the bodies immersed in a flow is shown in Fig. 6. Integration of p and of the longitudinal component of the shear stress at the boundaries γ_1 and γ_2 yields the following values for the drag coefficients: $C_1 = 1.49$ and $C_2 = -0.067$. This means that the rarefaction in the circulation cavity between the bodies enhances the overall pressure on the first cylinder (we recall that for a single cylinder, $C_d \approx 1.33$ at Re = 150) and simultaneously acts on the second cylinder in the direction opposite to the flow. Thus, if we rigidly connect both bodies, the overall drag coefficient of the tandem will be lower than that for a single cylinder.

Conclusions. An economical method of numerical simulation of a viscous separation flow around a system of bodies in a channel which is based on solving the Navier–Stokes equations in transformed variables has been developed. The calculation of the hydrodynamic fields was performed in three stages. First, with the aid of an iteration procedure the values of the stream function at the boundaries of the bodies are determined. In the second stage, an evolution problem of transfer and diffusion of vorticity (1), (2) is solved. In the final stage, problem (4) is solved with the aid of the found functions ψ and ω for fixed instants of time t for the Bernoulli variable, and the field of the pressure p is recovered. The method can be easily generalized to the cases of curvilinear channel walls and flow of a stream around an arbitrary number of bodies of arbitrary shape.

The flow around a pair of immovable and rotating circular channels in a channel has been calculated. Different cases of mutual disposition of the cylinders and directions of their rotation were considered. New qualitative characteristic features of flow and development of eddy structures in each case have been established.

The results of numerical simulation given in the article are mainly meant for illustrating the feasibilities of the proposed method. For a deeper understanding of the processes studied, it is necessary to carry out a series of computational experiments and ascertain the influence of the channel width, speed of the rotation of the bodies, and their location in the flow on the flow structure, drag coefficients, buoyancy, and the frequency of the shedding of vortices. A separate publication is planned where these results will be presented and analyzed.

This work was performed with financial support from the Russian Foundation for Fundamental Research (grants 03-01-00015, 03-01-96237, 04-01-00484).

NOTATION

b, auxiliary variable; B, Bernoulli variable; C_1 and C_2, drag coefficients of a pair of cylinders; C_d, drag of a single cylinder; D, calculation region; $\mathbf{f}$, vector of forces; G, arbitrary large number; H, half-width of the channel; i, ordinal number of the contour; j, number of the time layer of the computational scheme; L_1, L_2, and L, coordinates of the vertical boundaries of the calculation region and its length; $\mathbf{M}$, mass matrix; N, number of bodies immersed in a flow; n, normal to the boundary; p, pressure; Q, flow rate; Re, Reynolds number; s, arc of the contour; t, t_j (j = 1, 2, ...), time and time layer of the computational scheme; $\mathbf{V}$ and V, velocity vector and its modulus; u and v, components of the velocity vector $\mathbf{V}$; u_0, velocity at the channel inlet; v_i, speed of rotation of the ith cylinder; x, y, Cartesian coordinates; y_i^{c}, coordinate of the center of the ith cylinder; z, auxiliary variable; Γ_{top}, top wall of the channel; $|\gamma|$, length of the contour γ; γ_i (i = 1, 2, ..., N), boundaries of the bodies in a flow; ε, ξ, and φ, auxiliary variables; η, trial function; η_i (i = 1, 2, ..., N), auxiliary harmonic function; Λ, stiffness matrix; τ, step of the computational scheme in time; $\tilde{\varphi}$, approximate value of φ; ϕ, right side of the equation for ω on the time layer; ψ, stream function; ψ_i, boundary value of ψ on the contour i; ψ_0, stream function at the channel inlet; ψ_i^0, initial approximation for ψ_i; ω, vorticity; ω_i and ω_0, boundary values of ω. Superscript: c, center. Subscript: top, top.

REFERENCES

1. C. H. K. Williamson, Evolution of a single wake behind a pair of bluff bodies, *J. Fluid Mech.*, **159**, 1–18 (1985).
2. C. H. K. Williamson, Vortex dynamics in the cylinder wake, *Ann. Rev. Fluid Mech.*, **28**, 477–539 (1996).
3. M. M. Zdravkovich, Review of flow interface between two circular cylinders in various arrangements, *J. Fluids Eng. Trans. ASME*, **99**, No. 4, 618–633 (1997).
4. C. W. Ng, V. S. Y. Cheng, and N. W. M. Ko, Numerical study of vortex interactions behind two cylinders in bistable flow regime, *Fluid Dyn. Res.*, No. 19, 379–409 (1997).
5. T. Farrant, M. Tan, and W. G. Price, A cell boundary element method applied to laminar vortex shedding from circular cylinders, *Computers Fluids*, No. 30, 211–236 (2001).
6. D. L. Young, J. L. Huang, and T. I. Eldho, Simulation of laminar vortex shedding flow past cylinders using a coupled BEM and FEM model, *Comput. Meth. Appl. Mech. Eng.*, No. 190, 5975–5998 (2001).
7. A. B. Mazo and I. V. Morenko, Interaction of a viscous fluid flow with a rotating circular cylinder, in: *Models of Continuum Mechanics* [in Russian], Collected Papers of the N. I. Lobachevskii Mathematical Center, Vol. 27, Kazansk. Matem. Ob., Kazan' (2004), pp. 161–171.
8. A. B. Mazo and R. Z. Dautov, On the boundary conditions for Navier–Stokes equations in stream function–vorticity variables in simulation of a flow around a system of bodies, *Inzh.-Fiz. Zh.*, **78**, No. 4, 136–142 (2005).
9. P. J. Roache, *Computational Fluid Dynamics* [Russian translation], Mir, Moscow (1980).
10. C. A. J. Fletcher, *Computational Techniques for Fluid Dynamics* [Russian translation], Vol. 2, Mir, Moscow (1991).
11. A. B. Mazo and I. V. Morenko, Drag and rotational properties of cascades of circular cylinders at small and moderate Reynolds numbers, *Inzh.-Fiz. Zh.*, **77**, No. 2, 75–79 (2004).
12. A. V. Ermishin and S. A. Isaev (Eds.), *Control over Flows past Bodies with Vortex Cells as Applied to Flying Vehicles of Integral Arrangement* (*Numerical and Physical Modeling*) [in Russian], Izd. MGU, Moscow (2003).